

Abstract Self-propelled particle (SPP) systems are intrinsically out of equilibrium systems, where each individual particle converts energy into work to move in a dissipative medium. When interacting through a velocity alignment mechanism, and the medium acts as a momentum sink, even momentum is not conserved. In this scenario, a mapping into an equilibrium system seems unlikely. Here, we show that an entropy functional can be derived for SPPs with velocity alignment and density-dependent speed, at least in the (orientationally) disordered phase. This non-trivial result has important physical consequences. The study of the entropy functional reveals that the system undergoes phase separation above the orientational-order phase transition known to occur in SPP system with velocity alignment. Moreover, we indicate that the spinodal line is a function of the alignment sensitivity, diverging at the point where the orientational-order phase transition occurs. We show that density fluctuations also diverge as the orientational-order critical point is approached.

Motility-induced phase separation of active particles in the presence of velocity alignment

Julien Barré · Raphael Chétrite ·
Massimiliano Muratori · Fernando
Peruani

the date of receipt and acceptance should be inserted later

1 Introduction

Examples of biological interacting self-propelled particle (SPP) systems include animal groups [1,2], insect swarms [3,4], bacteria [5,6,7], and, at the microcellular scale, microtubules driven by molecular motors [8]. Even though most examples of SPPs come from biology, there exist non-living SPP systems. There are several ways of fabricating artificial SPPs. The self-propulsion of such particles typically requires an asymmetry in the particle: two distinct friction coefficients [9,10,11], light absorption coefficients [12,13,14,15], or catalytic properties [16,17,18,19,20] depending on whether energy injection is done through vibration, light emission, or chemical reaction, respectively. Interestingly, this asymmetry does not need to be an intrinsic particle property. Self-propelled Quincke rollers [21] as well as actively moving drops [22] are remarkable examples where the asymmetry results from a spontaneous symmetry breaking that sets the particle to move in a given direction.

At a theoretical level, we have learned in the recent years that the large-scale properties of SPP systems depend on few microscopic details. The symmetry associated to the self-propulsion mechanism of the particles, which can be either *polar* [23,24,25] or *apolar* [26], as well as the symmetry of the particle-particle interactions, that often occur via a velocity alignment mechanism, which can be either *ferromagnetic* [23,24] or *nematic* [26,25], play a fundamental role in the resulting self-organized patterns. Equally important is the dimension of the space where particles moves, whether this space is continuous (off-lattice) [23,24,26,25] or discrete (on lattice) [27,28,29,30], and whether particles move on a homogeneous or heterogeneous medium [31,32,33,34].

Another aspect of key importance, and central of the present study, is whether there exists a coupling between the speed and the density of the SP

particles. Notice that the importance lies on the existence of such coupling and not on the mere fact that the speed may fluctuate. In the context of SPPs with a velocity alignment, it has been shown first with a lattice model [35] and later on with an off-lattice model [36] that such a coupling induces spontaneous phase separation and a zoology of complex patterns. The most evident physical mechanism that can introduce a coupling between speed and density is simple volume exclusion effects as showed with a simple exclusion process on the lattice in [35] and with self-propelled disks [39] in an off-lattice model. The observed non-equilibrium phase separation can be traced back to the non-equilibrium *Motility Induced Phase Separation* (MIPS) introduced in the context of interacting run-and-tumble particles by J. Tailleur and M.E. Cates in [37,38]. In absence of an alignment mechanism, MIPS is a generic feature of active particles interacting by volume exclusion as shown in simulations with self-propelled disks [39,40,41] and spheres [42,43], and argued theoretically in [44,45]. One exciting aspect of the MIPS, as first pointed out in [37,38], is the remarkable similarity with equilibrium phase-separation, which allows the mapping between these non-equilibrium active systems with the analogous equilibrium systems.

The goal of the present study is to look at MIPS in the context of SPPs with a velocity alignment mechanism. Specifically, we want to understand the role played by the alignment mechanism in the phase separation process. Let us recall that SPP systems with a velocity alignment mechanism exhibit a phase transition from a disordered to an ordered phase. In the disordered phase, the large-scale behavior of the particles is diffusive as occurs for SPPs without a velocity alignment. Thus, we may hope that a mapping to an equilibrium scenario, as the one performed in [37,38], remains possible. We push for such an analogy as far as possible. To be exact, to the onset of the ordered phase.

Before starting, let us review briefly some of the most relevant theoretical results for (dried) SPP systems with velocity alignment and in the absence of density-dependent speed. The first hydrodynamical equations were derived based on symmetry arguments and contained all allowed terms by symmetry [46,47]. This initial studies provided a theoretical basis to understand the emergence of long-range order (LRO) in two dimensional systems with continuum symmetry as well as the presence of giant number fluctuations in the order phase. The drawback of these initial approaches is the impossibility of connecting the parameters of the hydrodynamic equations with those of the microscopic models. In [48], the macroscopic equations were derived from given microscopic equation. Such an approach revealed that the “parameters” of the hydrodynamic theory are in fact non-linear functions of the density. This has allowed to understand the emergence of macroscopic structures, such as bands, in this type of SPP systems [49,50]. For a detailed review, we refer the reader to [51]. Here, we just mentioned that macroscopic equations have been derived for ferromagnetic [46,47,48,51] and nematic velocity alignment [52] in the dilute approximation and close to the order-disorder critical point, with the exception of [53] and [54]. Even though we have now a fairly good quali-

tative understanding of the hydrodynamics of SPP systems (in homogeneous media), many open questions and fundamental problems remain unsolved.

The paper is organized as follows: we start by introducing the microscopic model we are interested in. The following section are devoted to the rather long computation which starts from the microscopic model and ends with the entropy functional describing the spatial density in the system. The main steps of the computation are outlined at the beginning of the third section. Finally, we draw some physical conclusions from the derived coarse-grained equations.

2 Model

We consider a system of N active particles, $i = 1, \dots, N$, moving in a two-dimensional space. The position of the i -th particle is given by $\mathbf{x}_i = (x_i, y_i)$ and what we refer to as its active velocity (AV) by $v(n_i)\mathbf{u}(\theta_i)$, where $\mathbf{u}(\theta_i) \equiv (\cos(\theta_i), \sin(\theta_i))$ defines the direction of the AV and $v(n_i) \equiv v_0\tilde{v}(n_i)$ its norm, with v_0 a constant and $\tilde{v}(n_i)$ a function that depends on n_i . The term n_i refers to the local density around the i -th particle. More specifically, $n_i = \sum_{j=1}^N g(|\mathbf{x}_i - \mathbf{x}_j|/R)$ where the function $g(\Delta/R)$, with $\Delta = |\mathbf{x}_i - \mathbf{x}_j|$ defines the interaction range. Finally, we consider an over-damped dynamics for the evolution of the $\mathbf{x}_i = (x_i, y_i)$ and θ_i such that the equations of motion of the i -th particle take the form:

$$\dot{\mathbf{x}}_i = v(n_i)\mathbf{u}(\theta_i) + \sqrt{2D_x}\boldsymbol{\sigma}_i(t) \quad (1)$$

$$\dot{\theta}_i = -\frac{\gamma}{n_i} \sum_{j=1}^N g(|\mathbf{x}_i - \mathbf{x}_j|/R) \sin(\theta_i - \theta_j) + \sqrt{2D_\theta}\eta_i(t). \quad (2)$$

The noise $\boldsymbol{\sigma}_i(t) = (\sigma_i^x(t), \sigma_i^y(t))$ and $\eta_i(t)$ for $i = 1, \dots, N$ are white, gaussian and uncorrelated noise with unit covariance. These noises represents a ‘‘bath’’ with very short time correlations or memory. The alignment sensitivity γ is not directly related to the fluctuation amplitude D_θ through an Einstein relation. A suitable option for the function g is to take $g(\Delta/R) = 1$ for $\Delta/R \leq 1$ and 0 otherwise, definition by which R defines the interaction range.

First, we write the equations of motion in adimensional form. Calling L the box size, we write $x_i = L\tilde{x}_i$, $y_i = L\tilde{y}_i$. We also rescale the time $t = \tilde{t}/D_\theta$, and adopt v_0 as the velocity scale. By using $\boldsymbol{\sigma}_i(\tilde{t}/D_\theta) = \sqrt{D_\theta}\boldsymbol{\sigma}_i(\tilde{t})$ and $\eta_i(\tilde{t}/D_\theta) = \sqrt{D_\theta}\eta_i(\tilde{t})$, we arrive to:

$$\frac{d\tilde{\mathbf{x}}_i}{d\tilde{t}} = \epsilon\tilde{v}(n_i)\mathbf{u}(\theta_i) + \epsilon\sqrt{2\tilde{D}_x}\boldsymbol{\sigma}_i(\tilde{t}) \quad (3)$$

$$\frac{d\theta_i}{d\tilde{t}} = -\frac{\bar{\gamma}}{n_i} \sum_{j=1}^N g((\tilde{\mathbf{x}}_i - \tilde{\mathbf{x}}_j)/\alpha) \sin(\theta_i - \theta_j) + \sqrt{2}\eta_i(\tilde{t}), \quad (4)$$

where we have introduced the dimensionless parameters $\bar{\gamma} = \gamma/D_\theta$, $\alpha = R/L$, $\epsilon = v_0/(LD_\theta)$, and $\tilde{D}_x = D_x D_\theta/v_0^2$, and so $n_i = \sum_{j=1}^N g((\tilde{\mathbf{x}}_i - \tilde{\mathbf{x}}_j)/\alpha)$. We

notice that $\tilde{D}_x = D_x D_\theta / v_0^2$ is the ratio between the passive (D_x) and active ($v_0^2/[2D_\theta]$) diffusion coefficient, which we consider to be of order ε^0 . From now on, we work with the adimensional equations and drop the $\tilde{\cdot}$ to simplify the notation. In the following, we will assume $\alpha \rightarrow 0$.

3 Main computation

As is clear from the scaling introduced through the parameter ε , we are interested in the situation where the dynamics over the angles θ_i is fast with respect to the spatial dynamics. Furthermore, we want to study the density of particles and their local mean orientation over large length scales. Our ultimate goal is to obtain a static large deviation principle yielding an entropy functional, which describes the fluctuations of the spatial empirical density, along the lines of [37,38], but accounting for the existence of a velocity alignment mechanism. To make the forthcoming computations easier to follow, we outline here the general scheme:

1. Write an effective equation for the phase space empirical density (that is in the variables x, y and θ), keeping the finite N fluctuations. This leads to a stochastic PDE with a noise term of order $1/\sqrt{N}$.
2. Take advantage of the time-scale separation to obtain a closed effective dynamics for the empirical density of the slow spatial variables x, y .
3. Write a functional Fokker-Planck equation for the macroscopic density field ρ .
4. Look for the stationary probability density of the macroscopic field ρ , under the asymptotic form $e^{NS[\rho]}$ and solve for S at leading order in N .

3.1 Dynamical equation for the phase space empirical density

We assume that N is large, but finite, and denote by $f_d(\mathbf{x}, \theta, t)$ the empirical density of particles in the 3D space given but $[x, y, \theta]$. The temporal evolution of $f_d(\mathbf{x}, \theta, t)$ is expressed in terms of the following stochastic partial differential equation:

$$\begin{aligned} \frac{\partial f_d}{\partial t} = & -\varepsilon \nabla \cdot (v(\rho(\mathbf{x}, t)) \mathbf{u}(\theta) f_d(\mathbf{x}, \theta, t)) + \frac{\bar{\gamma}}{\rho(\mathbf{x}, t)} \frac{\partial}{\partial \theta} \left(f_d(\mathbf{x}, \theta, t) \int d\theta' \sin(\theta - \theta') f_d(\mathbf{x}, \theta', t) \right) \\ & + \frac{\partial^2 f_d}{\partial \theta^2} + \varepsilon^2 D_x \nabla^2 f_d + \sqrt{\frac{2}{N}} \frac{\partial}{\partial \theta} \left(\eta(\mathbf{x}, \theta, t) \sqrt{f_d} \right) \\ & + \varepsilon \frac{\sqrt{2D_x}}{\sqrt{N}} \nabla \cdot \left(\boldsymbol{\sigma}(\mathbf{x}, \theta, t) \sqrt{f_d} \right), \end{aligned} \quad (5)$$

where $\eta(\mathbf{x}, \theta, t)$ and $\boldsymbol{\sigma}(\mathbf{x}, \theta, t)$ are gaussian noises, delta-correlated in time and space, and $\rho(\mathbf{x}, t)$ is the empirical spatial density defined by:

$$\rho(\mathbf{x}, t) = \int d\theta f_d(\mathbf{x}, \theta, t). \quad (6)$$

This can be shown at a formal level by following [55].

3.2 Averaging step - Time scale separation

We now take Fourier components of f_d of increasing order, stopping the expansion as soon as possible. This is a standard strategy, see e.g. [48]. Notice that finite N fluctuations are taken into account. We use the following notations: $\mathbf{P} = (P_x, P_y)$, with

$$\mathbf{P}(\mathbf{x}, t) = \int d\theta \mathbf{u}(\theta) f_d(x, y, \theta, t) \quad (7)$$

We neglect Fourier coefficients of higher order, and stress that it is consistent with a small ε expansion. Integrating Eq. (5) respectively over $d\theta$, $\cos\theta d\theta$ and $\sin\theta d\theta$, we obtain:

$$\frac{\partial \rho}{\partial t} = -\varepsilon \nabla \cdot (v\mathbf{P}) + \varepsilon^2 D_x \nabla^2 \rho + \varepsilon \frac{\sqrt{2D_x}}{\sqrt{N}} \nabla \cdot (\boldsymbol{\xi}(x, y, t)) \quad (8)$$

$$\frac{\partial \mathbf{P}}{\partial t} = -\frac{1}{2} \varepsilon \nabla \cdot (v\rho) + \left(\frac{\bar{\gamma}}{2} - 1\right) \mathbf{P} + \varepsilon^2 D_x \nabla^2 \mathbf{P} + \sqrt{\frac{2}{N}} \boldsymbol{\eta}(x, y, t) + O\left(\frac{\varepsilon}{\sqrt{N}}\right) \quad (9)$$

The noises are defined by

$$\eta_x(x, y, t) = \int d\theta \sin\theta \sqrt{f_d} \eta(x, y, \theta, t) \quad (10)$$

$$\eta_y(x, y, t) = - \int d\theta \cos\theta \sqrt{f_d} \eta(x, y, \theta, t) \quad (11)$$

$$\boldsymbol{\xi}(x, y, t) = \int d\theta \sqrt{f_d} \boldsymbol{\sigma}(x, y, \theta, t) \quad (12)$$

By construction, the noises are gaussian, delta-correlated in time and space. Furthermore

$$\langle \eta_x(x, y, t) \eta_x(x', y', t') \rangle \simeq \delta(x - x') \delta(y - y') \delta(t - t') \frac{1}{2} \rho(x, y, t) \quad (13)$$

$$\langle \eta_y(x, y, t) \eta_y(x', y', t') \rangle \simeq \delta(x - x') \delta(y - y') \delta(t - t') \frac{1}{2} \rho(x, y, t) \quad (14)$$

$$\langle \eta_x(x, y, t) \eta_y(x', y', t') \rangle \simeq 0 \quad (15)$$

$$\langle \boldsymbol{\xi}(x, y, t) \boldsymbol{\xi}(x', y', t') \rangle = \delta(x - x') \delta(y - y') \delta(t - t') \rho(x, y, t) \quad (16)$$

Consistently with our approximation, we have neglected in the noise correlation all Fourier coefficients beyond the first.

If $\bar{\gamma} \ll 2$, \mathbf{P} very quickly reaches its stationary value and remains small: particle motion is locally disordered, since the interaction promoting alignment is not strong enough to create a local orientational order. In this regime, we

can take the l.h.s. of Eq. (9) to be 0 in order to determine the stationary value of \mathbf{P} . Neglecting terms of order ε^2 and ε/\sqrt{N} , we obtain:

$$\mathbf{P} = \varepsilon \frac{1}{2(1 - \frac{\tilde{\gamma}}{2})} \nabla(v(\rho)\rho) + \sqrt{\frac{2}{N}} \frac{1}{1 - \frac{\tilde{\gamma}}{2}} \boldsymbol{\eta} \quad (17)$$

These computations are formal, and could in general lead to incorrect results: one should in particular be cautious about the meaning of the noise term, which is multiplicative. However, since we will eventually take a small noise limit (large N), this formal approach will correctly yield the leading order in N . We insert Eq.(17) into (8) and look for the long-time behavior of ρ by introducing a new time-scale $\tilde{t} = \varepsilon^2 t$:

$$\begin{aligned} \frac{\partial \rho}{\partial \tilde{t}} = & \frac{1}{2} \nabla \cdot \left(\frac{v}{1 - \frac{\tilde{\gamma}}{2}} \nabla[v(\rho)\rho] \right) + D_x \nabla^2 \rho \\ & + \frac{\sqrt{2D_x}}{\sqrt{N}} \nabla \cdot (\boldsymbol{\xi}(\mathbf{r}, t)) + \sqrt{\frac{2}{N}} \nabla \cdot \left(\frac{v}{1 - \frac{\tilde{\gamma}}{2}} \boldsymbol{\eta} \right), \end{aligned} \quad (18)$$

where again we have dropped the $\tilde{\cdot}$. Notice that due to the involved change of time-scale, all ε 's have disappeared of the final equation, and both noise terms give a contribution. The expansion in powers of ε is formally consistent. This means that one can hope that Eq. (18) is in some sense exact in the limit $N \rightarrow \infty$, $\varepsilon \rightarrow 0$.

Eq. (18) can be expressed in a more compact notations in the following way:

$$\frac{\partial \rho}{\partial \tilde{t}} = U[\rho](\mathbf{x}) + \frac{1}{\sqrt{N}} \nu(\mathbf{x}, t) \quad (19)$$

where

$$U[\rho](\mathbf{x}) = \frac{1}{2} \nabla \cdot \left(\frac{v(\rho)}{1 - \frac{\tilde{\gamma}}{2}} \nabla[v(\rho)\rho] \right) + D_x \nabla^2 \rho \quad (20)$$

and $\langle \nu(x, y, t) \nu(x', y', t') \rangle = D[\rho](\mathbf{x}, \mathbf{x}') \delta(t - t')$ with

$$D[\rho](\mathbf{x}, \mathbf{x}') = \partial_x \partial_{x'} [b[\rho](\mathbf{x}) \delta(\mathbf{x} - \mathbf{x}')] + \partial_y \partial_{y'} [b[\rho](\mathbf{x}) \delta(\mathbf{x} - \mathbf{x}')] \quad (21)$$

where

$$b[\rho] = 2D_x \rho + \frac{\rho v^2(\rho)}{(1 - \frac{\tilde{\gamma}}{2})^2}$$

We have combined here the two independent gaussian noise terms into a single one.

3.3 Functional Fokker-Planck equation

From Eq. (19), one can write a functional Fokker-Planck equation (see for details [56]) for the probability distribution of the density field $\mu_t[\rho]$:

$$\begin{aligned} \frac{\partial \mu_t}{\partial t} = & - \int d\mathbf{x} \frac{\delta}{\delta \rho(\mathbf{x})} (U[\rho](\mathbf{x}) \mu_t) \\ & + \frac{1}{2N} \int d\mathbf{x} \frac{\delta}{\delta \rho(\mathbf{x})} \left\{ \int d\mathbf{x}' D[\rho](\mathbf{x}, \mathbf{x}') \frac{\delta}{\delta \rho(\mathbf{x}')} \mu_t \right\} \end{aligned} \quad (22)$$

Note that we have here assumed an interpretation of the noise ν corresponding to Ito's convention. This has no consequence at leading order in N . We look for a stationary solution taking the asymptotic form

$$\mu[\rho] \sim e^{NS[\rho]} \quad (23)$$

and compute S at leading order in N . The drift U and the noise correlation D depend on ρ . However, we see that the relevant terms at leading order in N are obtained when the functional derivatives with respect to ρ act on μ_t rather than on U or D . This leads to the following equation for S :

$$\begin{aligned} \int U[\rho](\mathbf{x}) \frac{\delta S}{\delta \rho(\mathbf{x})} d\mathbf{x} = & \frac{1}{2} \left\{ \int d\mathbf{x} \left[\partial_x \frac{\delta S}{\delta \rho(\mathbf{x})} \int d\mathbf{x}' \partial_{x'} (b[\rho](\mathbf{x}') \delta(\mathbf{x} - \mathbf{x}')) \frac{\delta S}{\delta \rho(\mathbf{x}')} \right] \right. \\ & \left. + \int d\mathbf{x} \left[\partial_y \frac{\delta S}{\delta \rho(\mathbf{x})} \int d\mathbf{x}' \partial_{y'} (b[\rho](\mathbf{x}') \delta(\mathbf{x} - \mathbf{x}')) \frac{\delta S}{\delta \rho(\mathbf{x}')} \right] \right\} \\ = & -\frac{1}{2} \int d\mathbf{x} \nabla \cdot \left(b[\rho](\mathbf{x}) \nabla \frac{\delta S}{\delta \rho(\mathbf{x})} \right) \frac{\delta S}{\delta \rho(\mathbf{x})} \end{aligned} \quad (24)$$

By comparison and using the expression (20) for U , one sees that a sufficient condition to find S is to solve the equation

$$\frac{1}{2} b[\rho] \nabla \cdot \frac{\delta S}{\delta \rho(\mathbf{x})} = -\frac{1}{2} \frac{v(\rho)}{1 - \frac{\tilde{\gamma}}{2}} \nabla(\rho v(\rho)) - D_x \nabla \rho \quad (25)$$

Formally, it can be shown that this expression represents the equilibrium condition for $\mu[\rho]$, that is the condition for a zero-flux solution of the functional Fokker-Planck equation, Eq. (22). Equivalently, this corresponds to the reversibility of the dynamics given by Eq. (19) with respect to the density $\mu[\rho]$. We look for a solution S , which is a local functional of ρ , and of the form:

$$S[\rho] = \int d\mathbf{x} s(\rho(\mathbf{x})) \quad (26)$$

where the entropy density s is a real function to be determined. One finds

$$s''(\rho) = - \left(\frac{v^2(\rho) + \rho v(\rho) v'(\rho)}{(1 - \frac{\tilde{\gamma}}{2}) b[\rho]} + \frac{2D_x}{b[\rho]} \right) \quad (27)$$

When the integration of Eq. (27) is possible, the function s can be explicitly retrieved. This is the main result of this article. The physical consequences are discussed in the following section.

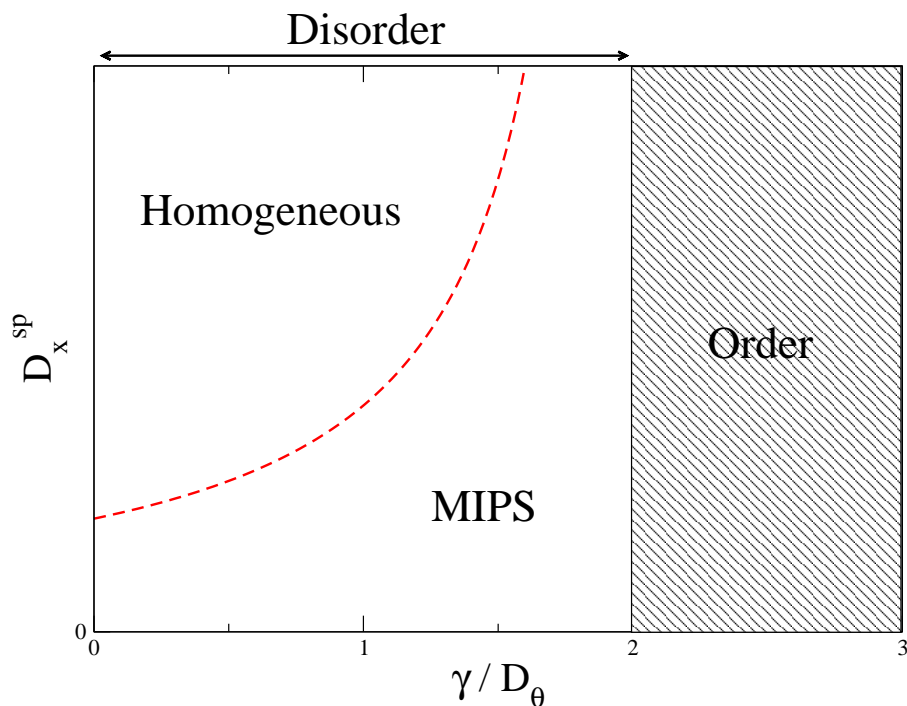


Fig. 1 Sketch of phase diagram. The figure indicates that the transition between the (orientationally) disordered and ordered phase is controlled by the ratio $\bar{\gamma} = \gamma/D_\theta$. In the disorder phase, the red curve represents the spinodal line that diverges as the critical orientational order point is approached. As we come close to this critical point density fluctuations diverge (see text). Above the red curve there is only one homogeneous phase, while below the system phase separates, i.e., the homogeneous phase is no longer stable. It has been shown that the ordered phase can exhibit a zoo of patterns, see [35,36]. In the sketch we have assumed that $v(\rho) = v_0 \exp(-\lambda\rho)$, with λ large enough to allow MIPS.

4 Physical discussion and final remarks

Let us review the results we obtained. Our starting point was Eq. (5). This equation becomes an exact description of the system in the limite of large N and large densities. Thus, for finite but large N , Eq. (5) should provide a good description for the particle density of a system whose microscopic dynamics is given by Eqs. (1) and (2). Our goal has been to derive an entropy-like functional for the particle density. In order to do that, we expressed the polar order \mathbf{P} as function of the density ρ and its gradients. We make use of the fast relaxation of \mathbf{P} with respect of the temporal evolution of ρ . Such a separation of time-scales played a crucial role in the derivation of the entropy functional. Strictly speaking, this is true in the disordered phase. From Eq. (9), we can easily see that the onset of local (orientational) order occurs for $\bar{\gamma}/2 - 1 > 0$, that is, when the angular diffusion D_θ is such that $D_\theta < \gamma/2$. This means that

the entropy functional, given by Eqs. (26) and (27), is valid for $D_\theta > \gamma/2$, see solid vertical line in Fig. 1.

To understand the physical meaning of the derived equations, let us adopt a concrete functional form for $v(\rho)$, e.g. $v(\rho) = v_0 \exp(-\lambda\rho)$. Notice that the qualitative features discussed below do not depend on the precise functional form for $v(\rho)$, provided it is decreasing. Phase separation, below the spinodal line, implies that an homogeneous phase cannot be stable. The spinodal can be found solving $s''(\rho) = 0$, using expression Eq. (27). One finds

$$e^{-2\lambda\rho}(\lambda\rho - 1) = \frac{D_x \left(1 - \frac{\bar{\gamma}}{2}\right)}{v_0^2} \quad (28)$$

For ρ, λ such that $\lambda\rho > 1$, Eq. (28) is represented by the red dashed line in Fig. 1. Above this line, the homogeneous solution is stable; below it, spinodal decomposition (Motility-Induced Phase Separation) occurs. Notice that this line, which corresponds to a dynamical instability, can also be obtained by linearizing Eq. (19), without noise, around a spatially homogeneous solution. Eq. (27) also gives access to the metastable regions around the spinodal line. Figure 1 shows that the critical spatial diffusion D_x^{sp} below which the homogeneous solution is unstable strongly depends on $\bar{\gamma} = \gamma/D_\theta$: the divergence of D_x^{sp} is connected to the term in $1/(1 - \bar{\gamma}/2)$ in Eq. (20). This high sensitivity of the spinodal line to the alignment strength, i.e. γ , is inline with results obtained in simulations [35]. Notice that at this level of approximation, D_x does not affect the orientational order critical point, while γ and D_θ play a role on both, the disordered and ordered phase. Now, let us turn to the analysis of density fluctuations related to the noise term present in Eq. (19). From Eq. (27), we learn that in the homogeneous phase, an alignment interaction $\gamma > 0$ makes s'' smaller in absolute value, and thus it increases the density fluctuations. Notice that density fluctuations diverge for $s'' \rightarrow 0$. This occurs on the spinodal line, as well as in the MIPS phase, as we approach the orientational order critical point, i.e. $\gamma \rightarrow 2D_\theta$. It is worth noticing that for $D_x = 0$, γ has no influence on the phase diagram shown in Fig. 1, while it still has on the density fluctuations.

In summary, our calculations indicate that phase separation can occur in the disorder phase with the alignment strength – more specifically with the “distance” to the orientational order critical point – controlling the position of the spinodal line involved in the MIPS as well as the size of density fluctuations. In short, we have generalized the approach of [37, 38] in order to account for the presence of a velocity alignment mechanism. While the nature of the described phase separation remains a MIPS as observed in non-aligning systems [39, 40, 41, 42, 43, 44, 45], this does not exclude that in the orientationally ordered phase, phase separation can be of a different nature as suggested in [57].

acknowledgements We acknowledge enlightening discussions with O. Dauchot, P. Degond, and J. Tailleur and financial support from the PEPS-PTI “Anomalous fluctuations in the collective motion of self-propelled particles”. The suggestion by J. Tailleur of adding a white noise to Eq.(1) has proved to

be very fruitful for the present study. FP thanks the Kavli Institute for Theoretical Physics (University of California, Santa Barbara) and the organizers of the bioacter14 program for hospitality and financial support.

References

1. A. Cavagna et al., Proc. Natl. Acad. Sci. **107**, 11865 (2010).
2. K. Bhattacharya and T. Vicsek, New J. Phys. **12**, 093019 (2010).
3. J. Buhl et al., Science **312**, 1402 (2006).
4. P. Romanczuk, I.D. Couzin, and L. Schimansky-Geier, Phys. Rev. Lett. **102**, 010602 (2009).
5. H.P. Zhang et al., Proc. Natl. Acad. Sci. **107**, 13626 (2010).
6. F. Peruani et al., Phys. Rev. Lett. **108**, 098102 (2012).
7. J. Starruss et al., Interface Focus **2**, 774 (2012).
8. V. Schaller et al., Nature **467**, 73 (2010).
9. A. Kudrolli et al., Phys. Rev. Lett. **100**, 058001 (2008).
10. J. Deseigne, O. Dauchot, and H. Chaté, Phys. Rev. Lett. **105**, 098001 (2010).
11. C. A. Weber, T. Hanke, J. Deseigne, S. Leonard, O. Dauchot, E. Frey, and H. Chaté, Phys. Rev. Lett. **110**, 208001 (2013).
12. H.-R. Jiang, N. Yoshinaga, and M. Sano, Phys. Rev. Lett. **105**, 268302 (2010).
13. R. Golestanian, Phys. Rev. Lett. **108**, 038303 (2012).
14. Theurkauff et al., Phys. Rev. Lett. **108**, 268303 (2012).
15. Palacci et al., Science **339**, 936 (2013).
16. W. Paxton et al., J. Am. Chem. Soc., **126**, 13424 (2004).
17. N. Mano and A. Heller, J. Am. Chem. Soc. **127**, 11574 (2005).
18. G. Rückner and R. Kapral, Phys. Rev. Lett. **98**, 150603 (2007).
19. J. Howse et al., Phys. Rev. Lett. **99**, 048102 (2007).
20. R. Golestanian, T.B. Liverpool, and A. Ajdari, Phys. Rev. Lett. **94**, 220801 (2005).
21. A. Bricard et al., Nature **503**, 95 (2013).
22. S. Thutupalli, R. Seemann, S. Herminghaus, New J. Phys. **13**, 073021 (2011).
23. T. Vicsek et al., Phys. Rev. Lett. **75**, 1226 (1995).
24. G. Grégoire and H. Chaté, Phys. Rev. Lett. **92**, 025702 (2004).
25. F. Peruani, A. Deutsch, and M. Bär, Eur. Phys. J-Spec. Top., **157**, 111 (2008); F. Ginelli et al., Phys. Rev. Lett. **104**, 184502 (2010).
26. H. Chaté, F. Ginelli and R. Montagne, Phys. Rev. Lett. **96**, 180602 (2006).
27. H.J. Bussemaker, A. Deutsch, and E. Geigant, Phys. Rev. Lett. **78**, 5018 (1997).
28. Z. Csahók and T. Vicsek, Phys. Rev. E **52**, 5297 (1995).
29. O.J. O’Loan and M.R. Evans, J. Phys. A: Math. Gen. **32**, 99 (1999).
30. J.R. Raymond and M.R. Evans, Phys. Rev. E **73**, 036112 (2006).
31. O. Chepizhko, E. Altmann, and F. Peruani Phys. Rev. Lett. **110**, 238101 (2013).
32. O. Chepizhko and F. Peruani Phys. Rev. Lett. **111**, 160604 (2013).
33. C. Reichhardt and C.J. Olson Reichhardt, arXiv:1402.3260 (2014).
34. David A. Quint, Ajay Gopinathan, arXiv:1302.6564 (2013).
35. F. Peruani et al., Phys. Rev. Lett. **106**, 128101 (2011).
36. F. D. C. Farrell et al., Phys. Rev. Lett. **108**, 248101(2012).
37. J. Tailleur and M. E. Cates, Phys. Rev. Lett. **100**, 218103 (2008).
38. M.E. Cates and J. Tailleur, Europhys. Lett. **101**, 20010 (2013).
39. Y. Fily and M.C. Marchetti, Phys. Rev. Lett. **108**, 235702 (2012).
40. G. Redner, M.F. Hagan, A. Baskaran, Phys. Rev. Lett. **110**, 055701 (2013).
41. Y. Fily, S. Henkes, and M.C. Marchetti, Soft Matter (2014).
42. B.M. Mognetti et al. Phys. Rev. Lett. **111**, 245702 (2013).
43. A. Wysocki, R.G. Winkler, G. Gompper, arXiv:1308.6423 (2013)
44. J. Stenhammar et al., Phys. Rev. Lett. **111**, 145702 (2013).
45. T. Speck et al., arXiv:1312.7242 (2013).
46. J. Toner and Y. Tu, Phys. Rev. Lett. **75**, 4326 (1995).
47. J. Toner and Y. Tu, Phys. Rev. E **58**, 4828 (1998).

48. E. Bertin, M. Droz and G. Grégoire J. Phys. A 42, 445001 (2009).
49. S. Mishra, A. Baskaran, and M.C. Marchetti, Phys. Rev. E 81, 061916 (2010).
50. J-B. Caussin et al., arXiv:1401.1315 (2014).
51. M. C. Marchetti et al., Rev. Mod. Phys. **85**, 1143 (2013)
52. A. Peshkov et al., Phys. Rev. Lett. **109**, 268701 (2012).
53. T. Ihle, Phys. Rev. E **83**, 030901 (2011).
54. P. Degond and S. Motsch, Math. Models Methods Appl. Sci. **18**, 1193 (2008).
55. D.S. Dean, J. Phys. A: Math. Gen. **29**, L613 (1996).
56. C. W. Gardiner, *Handbook of stochastic methods* (Springer, Heidelberg, 2004).
57. F. Peruani and M. Bär, New J. Phys. **15**, 065009 (2013).